

**An Investigation of Discretization Errors for
Mesh Centered Finite Difference Approximations
to the Transport Equation Using a Spherical
Harmonic Expansion of the Flux**

July 1997

**O-arai Engineering Center
Power Reactor and Nuclear Fuel Development Corporation**

複製又はこの資料の入手については、下記にお問い合わせ下さい。

〒311-13 茨城県東茨城郡大洗町成田町4002

動力炉・核燃料開発事業団

大洗工学センター

システム開発推進部技術管理室

Inquiries about copyright and reproduction should be addressed to : Technology Management Section, O-arai Engineering Center, Power Reactor and Nuclear Fuel Development Corporation 4002 Narita-machi, O-arai-machi, Higashi-Ibaraki, Ibaraki-Ken 311-13, Japan.

動力炉・核燃料開発事業団

(Power Reactor and Nuclear Fuel Development Corporation) 1997

**An Investigation of Discretization Errors for
Mesh Centered Finite Difference Approximations
to the Transport Equation Using a Spherical
Harmonic Expansion of the Flux**

J. K. Fletcher*

ABSTRACT

The multigroup Transport Equation for the flux column vector $\Psi(\mathbf{r}, \Omega)$ at location \mathbf{r} in the direction of unit vector Ω ,

$$\Omega \cdot \nabla \Psi(\mathbf{r}, \Omega) + \sigma_t(\mathbf{r}) \Psi(\mathbf{r}, \Omega) = \int_{\Omega_1} \left(\sigma_s(\mathbf{r}, \Omega_1, \Omega) + \frac{v\sigma_f(\mathbf{r})}{k} \right) \Psi(\mathbf{r}, \Omega_1) d\Omega_1 + Q(\mathbf{r}, \Omega)$$

where $\sigma_t(\mathbf{r})$, $\sigma_s(\mathbf{r}, \Omega_1, \Omega)$ and $v\sigma_f(\mathbf{r})$ are the total, scatter from Ω_1 to Ω and production cross section matrices respectively with k a criticality constant and $Q(\mathbf{r}, \Omega)$ any external source, is solved using an expansion of the flux in spherical harmonics. That is

$$\Psi(\mathbf{r}, \Omega) = \sum_{l=0}^N (2l+1) \sum_{m=0}^l P_l^m(\cos \theta) (\psi_{lm}(\mathbf{r}) \cos(m\phi) + \gamma_{lm}(\mathbf{r}) \sin(m\phi))$$

with $P_l^m(\cos \theta)$ the associated Legendre polynomial of order l, m and θ the axial and ϕ azimuthal angles of Ω respectively. N is the order of the approximation denoted by PN .

Using the independence of the polynomials combined with trigonometric functions thus forming spherical harmonics and their recurrence relations first order differential equations are found for moments $\psi_{lm}(\mathbf{r})$ and $\gamma_{lm}(\mathbf{r})$. Odd l terms are eliminated to give a linked second order system which is solved by standard finite difference methods used for the diffusion equation.

To reduce mesh effects higher order difference terms are retained in the numerical approximation made to the second order system.

Finally results are presented showing that mesh effects can be greatly reduced thus enabling finite difference results to be compared directly with other solutions particularly those obtained by Monte Carlo methods.

* PNC International Fellow, Reactor Physics Research Section, Advanced Technology Division, O-arai, PNC, Japan.

球面調和関数展開を用いた輸送方程式における 有限差分近似によるメッシュ誤差低減の研究

J. K. フレッチャー*

要旨

位置 \mathbf{r} 、単位方向ベクトル Ω の中性子束を $\Psi(\mathbf{r}, \Omega)$ と定義すると、多群輸送方程式は次式で表される。

$$\Omega \cdot \nabla \Psi(\mathbf{r}, \Omega) + \sigma_t(\mathbf{r}) \Psi(\mathbf{r}, \Omega) = \int_{\Omega_1} \left(\sigma_s(\mathbf{r}, \Omega_1, \Omega) + \frac{v\sigma_f(\mathbf{r})}{k} \right) \Psi(\mathbf{r}, \Omega_1) d\Omega_1 + Q(\mathbf{r}, \Omega)$$

ただし、 $\sigma_t(\mathbf{r})$ 、 $\sigma_s(\mathbf{r}, \Omega_1, \Omega)$ 、 $v\sigma_f(\mathbf{r})$ はそれぞれ、全断面積、方向 Ω_1 から Ω への散乱断面積、生成断面積を表し、また、 k は臨界係数を、 $Q(\mathbf{r}, \Omega)$ は外部中性子源を表す。

そして、この方程式を次の球面調和関数展開を用いて解く。

$$\Psi(\mathbf{r}, \Omega) = \sum_{l=0}^N (2l+1) \sum_{m=0}^l P_l^m(\cos\theta) (\psi_{lm}(\mathbf{r}) \cos(m\phi) + \gamma_{lm}(\mathbf{r}) \sin(m\phi))$$

ここで、 $P_l^m(\cos\theta)$ はオーダー l, m のルジャンドル陪関数で、 θ と ϕ はそれぞれ方向 Ω の仰角及び方位角を表す。 N は PN 近似の次数を表す。

三角関数の多項式である球面調和関数の直交性と漸化式を用いることにより、展開係数 $\psi_{lm}(\mathbf{r})$ と $\gamma_{lm}(\mathbf{r})$ に関する1階の微分方程式が導かれる。 l が奇数の項を消去することにより、拡散方程式の場合に用いられるような通常の有限差分法により解くことの可能な、2次の微分方程式が導かれる。

メッシュ誤差低減は、その記述式の高次の差分項を保持したまま、2次式を用いて数値的に近似することにより行われる。

当手法の採用により、メッシュ誤差は大幅に低減され、他の手法、特にモンテカルロ法により得られたものに匹敵する結果を直接計算することが可能となった。

*: 基盤技術開発部 炉心技術開発室 国際特別研究員

CONTENTS

	page
ABSTRACT	i
要旨	ii
CONTENTS	iii
List of Tables	iv
List of Figures	v
Chapter 1. INTRODUCTION	1
Chapter 2. EQUATIONS FOR SOLUTION	1
Chapter 3. NUMERICAL APPROXIMATION TO THE EQUATIONS FOR SOLUTION	4
Chapter 4. BOUNDARY CONDITIONS	8
Chapter 5. TRANSPORT THEORY SOLUTION ALGORITHM.	10
Chapter 6. MESH CORRECTION TERMS	10
Chapter 7. TEST CASES	12
Chapter 8. CONCLUSIONS	14
REFERENCES	15
Appendix 1 FORTRAN CODE TO CALCULATE THE SECOND ORDER SYSTEM	21
Appendix 2 P3 EQUATIONS FOR XYZ GEOMETRY	23
Appendix 3 Cross Section Data for the XYZ Geometry Tests	24

List of Tables

- Table 1 Eigenvalues for the Small FBR Control Rod Out
- Table 2 Eigenvalues for the Small FBR Control Rod Half In
- Table 3 Eigenvalues for the Large FBR Control Rod In
- Table 4 Eigenvalues for the Large FBR Control Rod Out

List of Figures

- Figure 1 Definition of r and Ω
- Figure 2 A typical mesh in XYZ Geometry
- Figure 3 Small FBR Test Problem
- Figure 4 Large FBR Test Problem

Chapter 1. INTRODUCTION

A previous report⁽¹⁾ presented a method of reducing the discretization errors made when solving the multigroup diffusion equation using mesh centered finite difference approximations. Essentially second order differential terms were retained as a perturbation in the numerical representation leading to a much reduced dependence of eigenvalue and fluxes on mesh size.

In this work the approach is extended to the transport equation which although a first order differential equation because, in contrast to diffusion theory, flux angular dependence is modeled usually cannot be solved easily. The technique adopted expands the flux in unnormalised spherical harmonics and then derives a second order differential system of diffusion-like equations which can be solved using the well established algorithms used in diffusion theory⁽²⁾.

Chapter 2 gives the basic theory of the transport solution and Chapter 3 shows how the difference approximation is derived. After a specification of external boundary conditions a description of the solution algorithm follows with the mesh correction procedure being given in Chapter 6. After details of test cases the report ends with a Conclusions section in which future developments are also discussed.

Chapter 2. EQUATIONS FOR SOLUTION

The multigroup Transport Equation for the flux column vector $\Psi(\mathbf{r}, \Omega)$ at location \mathbf{r} in the direction of unit vector Ω , in the form⁽³⁾

$$\Omega \cdot \nabla \Psi(\mathbf{r}, \Omega) + \sigma_t(\mathbf{r}) \Psi(\mathbf{r}, \Omega) = \int_{\Omega_1} \left(\sigma_s(\mathbf{r}, \Omega_1, \Omega) + \frac{v\sigma_f(\mathbf{r})}{k} \right) \Psi(\mathbf{r}, \Omega_1) d\Omega_1 + Q(\mathbf{r}, \Omega) \quad (1)$$

where $\sigma_t(\mathbf{r})$, $\sigma_s(\mathbf{r}, \Omega_1, \Omega)$ and $v\sigma_f(\mathbf{r})$ are the total, scatter from Ω_1 to Ω and production cross section matrices respectively with k a criticality constant and $Q(\mathbf{r}, \Omega)$ any external source, is solved using an expansion of the flux in spherical harmonics. That is

$$\Psi(\mathbf{r}, \Omega) = \sum_{l=0}^N (2l+1) \sum_{m=0}^l P_l^m(\cos \theta) (\psi_m(\mathbf{r}) \cos(m\phi) + \gamma_m(\mathbf{r}) \sin(m\phi)) \quad (2)$$

with $P_l^m(\cos \theta)$ the associated Legendre polynomial of order l, m and θ the axial and ϕ the azimuthal angles of Ω respectively as shown in Figure 1. N is the order of the expansion usually taken to be odd. The flux is continuous everywhere with the vacuum boundary condition of no incoming flux and satisfies a reflective condition if required. Flux continuity is taken to imply that moments, $\psi_m(\mathbf{r})$ and $\gamma_m(\mathbf{r})$ in expansion (2), are continuous, particularly across material interfaces, because spherical harmonics are independent and this approach is

widely accepted⁽⁴⁾. However other workers⁽⁵⁾ employ a different technique based on neutron flow conservation leading to extremely complicated numerical equations for solution.

In terms of θ and ϕ , $\Omega \cdot \nabla$ becomes in XYZ geometry

$$\begin{aligned} \Omega \cdot \nabla &= \frac{\partial}{\partial s} = \frac{\partial z}{\partial s} \frac{\partial}{\partial z} + \frac{\partial x}{\partial s} \frac{\partial}{\partial x} + \frac{\partial y}{\partial s} \frac{\partial}{\partial y} \\ &= \cos \theta \frac{\partial}{\partial z} + \sin \theta \cos \phi \frac{\partial}{\partial x} + \sin \theta \sin \phi \frac{\partial}{\partial y} \end{aligned} \quad (3)$$

as can be deduced from Figure 1 on realizing that it is just the derivative of the flux along the direction Ω .

$\sigma_i(\mathbf{r}, \Omega_i, \Omega)$ is assumed to be a function only of the angle between incident and emergent directions that is $\Omega_i \cdot \Omega = \cos \theta_0$, say so that the following expansion in Legendre polynomials may be made.

$$\sigma_i(\mathbf{r}, \cos \theta_0) = \frac{1}{4\pi} \sum_{l=0}^{\infty} (2l+1) \sigma'_i(\mathbf{r}) P_l(\cos \theta_0) \quad (4)$$

The associated Legendre polynomials satisfy the following recurrence relations

$$(2l+1) \cos \theta P_l^m(\cos \theta) = (l-m+1) P_{l+1}^m(\cos \theta) + (l+m) P_{l-1}^m(\cos \theta) \quad (5)$$

and

$$\begin{aligned} (2l+1) \sin \theta P_l^m(\cos \theta) &= P_{l+1}^{m+1}(\cos \theta) - P_{l-1}^{m+1}(\cos \theta) \\ &= (l+m-1)(l+m) P_{l-1}^{m-1}(\cos \theta) - (l-m+1)(l-m+2) P_{l+1}^{m-1}(\cos \theta) \end{aligned} \quad (6)$$

On inserting expansions (2) and (4) in equation (1) and using the recurrence relations (5) and (6) along with the addition formula

$$P_l(\cos \theta_0) = \sum_{m=0}^l (2-\delta_m^0) \frac{(l+m)!}{(l-m)!} P_l^m(\cos \theta) P_l^m(\cos \theta_0) \cos m(\phi - \phi_0) \quad (7)$$

where θ and ϕ are the angles for direction Ω , the subscripted values being for Ω_i and δ_i^j is the Kronecker delta function having value unity if $i=j$ and zero otherwise then, since the Associated Legendre polynomials multiplied by trigonometric functions that is unnormalised spherical harmonics are independent, the following moment equations result

$$\begin{aligned}
 & (l-m)\frac{\partial\psi_{l-1m}}{\partial z} + (l+m+1)\frac{\partial\psi_{l+1m}}{\partial z} + \frac{1}{2}\left(\frac{\partial\psi_{l-1m-1}}{\partial x} - \frac{\partial\gamma_{l-1m-1}}{\partial y} - \frac{\partial\psi_{l+1m-1}}{\partial x} + \frac{\partial\gamma_{l+1m-1}}{\partial y}\right) \\
 & + \frac{1}{2}\left((l-m)(l-m-1)\left(-\frac{\partial\psi_{l-1m+1}}{\partial x} - \frac{\partial\gamma_{l-1m+1}}{\partial y}\right) + (l+m+1)(l+m+2)\left(\frac{\partial\psi_{l+1m+1}}{\partial x} + \frac{\partial\gamma_{l+1m+1}}{\partial y}\right)\right) \\
 & + (2l+1)\sigma_l\psi_{lm} = (2l+1)Q_{lm}
 \end{aligned} \tag{8}$$

and

$$\begin{aligned}
 & (l-m)\frac{\partial\gamma_{l-1m}}{\partial z} + (l+m+1)\frac{\partial\gamma_{l+1m}}{\partial z} + \frac{1}{2}\left(\frac{\partial\psi_{l-1m-1}}{\partial y} + \frac{\partial\gamma_{l-1m-1}}{\partial x} - \frac{\partial\psi_{l+1m-1}}{\partial y} - \frac{\partial\gamma_{l+1m-1}}{\partial x}\right) \\
 & + \frac{1}{2}\left((l-m)(l-m-1)\left(\frac{\partial\psi_{l-1m+1}}{\partial y} - \frac{\partial\gamma_{l-1m+1}}{\partial x}\right) + (l+m+1)(l+m+2)\left(-\frac{\partial\psi_{l+1m+1}}{\partial y} + \frac{\partial\gamma_{l+1m+1}}{\partial x}\right)\right) \\
 & + (2l+1)\sigma_l\gamma_{lm} = (2l+1)Q'_{lm}
 \end{aligned} \tag{9}$$

$\sigma_l = \sigma_l(\mathbf{r}) - \sigma'_l(\mathbf{r}) - \frac{v\sigma_l(\mathbf{r})}{k}\delta_l^0$ and dependence on space variables in equations (8) and(9) is understood. Q_{lm} and Q'_{lm} result from the expansion of any external source in a manner similar to the flux.

The next step is to eliminate odd l terms, a process normally carried out by a computer program as the equations are quite complicated. Appendix 1 shows the small FORTRAN code used for this process and Appendix 2 gives the second order equations for an expansion up to $N=3$. N is usually chosen to be odd since an even value means second order equations for odd l result and the scalar flux, which is needed for reaction rate calculations, has to be separately evaluated by interpolation. The process may be difficult because although odd moments are continuous they may not be smooth, particularly across material interfaces where their derivatives exhibit discontinuities.

Appendix 2 shows quite clearly the system of equation's diffusion-like nature for the l, m differentials with other moments constituting source terms.

The second order equations may be written symbolically as

$$a_{lmn}^{i'm'n'}\frac{\partial^2\psi_{lmn}}{\partial x_i^2} + b_{lmn}^{i'm'n'}\frac{\partial^2\psi_{lmn}}{\partial x_i\partial x_k} + (2l+1)\sigma_l\psi_{lmn} = (2l+1)Q_{lmn} \tag{10}$$

where repeated primed subscripts and superscripts obey the summation convention so that l takes the values $l-2, l$ and $l+2$ while m goes from $m-2$ to $m+2$. $n=1$ implies ψ_{lm} and $n=2$, γ_{lm} . x_i signifies the variable x , x_2 denotes y and x_3, z . Equation (10) is intended mainly as a guide and a more detailed formulation will be given in Chapter 3.

Chapter 3 NUMERICAL APPROXIMATION TO THE EQUATIONS FOR SOLUTION

As in earlier work⁽¹⁾ the basis of the numerical approximation is Taylor's expansion which for a continuous function, $f(x,y,z)$, with continuous derivatives may be written

$$f(x + \delta x, y + \delta y, z + \delta z) = f(x, y, z) + \sum_{n=1}^{\infty} \sum_{\substack{i,j,k \\ i+j+k=n}} \frac{\delta x^i \delta y^j \delta z^k}{i!j!k!} \frac{\partial^n f(x, y, z)}{\partial x^i \partial y^j \partial z^k} \quad (11).$$

First the problem has a regular mesh imposed on it as shown in Figure 2 where the boundaries of mesh regions coincide with changes of material then equation (10) is integrated over each volume V_{ijk} and becomes

$$\begin{aligned} & \sum_{p=1}^6 \int_{S_p} \left(a_{lmni}^{i'm'n'} \frac{\partial \psi_{i'm'n'}}{\partial x_i} + b_{lmnji}^{i'm'n'} \frac{\partial \psi_{i'm'n'}}{\partial x_j} + b_{lmnik}^{i'm'n'} \frac{\partial \psi_{i'm'n'}}{\partial x_k} \right) dS_p + \int_{V_{ijk}} (2l+1) \sigma_l \psi_{lmn} dV \\ & = \int_{V_{ijk}} (2l+1) Q_{lmn} dV \end{aligned} \quad (12),$$

p denoting the cell boundaries in some order.

Approximations to the foregoing integrals are made using values of the flux moments at the mesh region centers. Thus, letting f_{ijk} denote a flux moment value at meshpoint ijk , the volume term takes the form

$$\begin{aligned} & \int_{V_{ijk}} (2l+1) (\sigma_l)_{ijk} \left(f_{ijk} + \left(x \frac{\partial}{\partial x} + y \frac{\partial}{\partial y} + z \frac{\partial}{\partial z} \right) f_{ijk} \right. \\ & \left. + \frac{1}{2} \left(x^2 \frac{\partial^2}{\partial x^2} + 2xy \frac{\partial^2}{\partial x \partial y} + 2xz \frac{\partial^2}{\partial x \partial z} + y^2 \frac{\partial^2}{\partial y^2} + 2yz \frac{\partial^2}{\partial y \partial z} + z^2 \frac{\partial^2}{\partial z^2} \right) f_{ijk} + \dots \right) dV \end{aligned} \quad (13)$$

or after integration because odd terms become zero

$$(2l+1) (\sigma_l)_{ijk} V_{ijk} \left(f_{ijk} + \frac{1}{24} \left(\alpha_i^2 \frac{\partial^2}{\partial x^2} + \beta_j^2 \frac{\partial^2}{\partial y^2} + \gamma_k^2 \frac{\partial^2}{\partial z^2} \right) f_{ijk} + \dots \right) \quad (14).$$

To deal with mesh boundary terms it is more convenient to begin with the first order equations (8) and (9) which may be written compactly as

$$c_{lmn,p}^{i'm'n'} \frac{\partial \psi_{i'm'n'}}{\partial x_p} + (2l+1)\sigma_i \psi_{lmn} = (2l+1)Q_{lmn} \quad (15)$$

on using the summation convention defined for relation (10) with $l = l \pm 1$ and $m = m, m \pm 1$. Also subscript p may be taken as summed but this just implies many coefficients are zero. The equivalent to relation (12) then takes the form

$$\sum_{p=1}^3 \int_{S_p} \pm c_{lmn,p}^{i'm'n'} \psi_{i'm'n'} dS^{\pm p} + \int_{V_{ijk}} (2l+1)\sigma_i \psi_{lmn} dV = \int_{V_{ijk}} (2l+1)Q_{lmn} dV \quad (16).$$

Superscript $\pm p$ denotes the surface in the positive or negative direction along axis p as defined for equation (10) so that S^{\pm} is the cell boundary shown in Figure 2. The moments integrated over the surfaces $S^{\pm p}$ all have odd l , hence the continuity of these odd l terms can be used to derive analogous relations to those for Diffusion theory(1).

Assuming there is no anisotropic external source the continuity of odd moments implies that

$$\frac{1}{\sigma_i} c_{lmn,p}^{i'm'n'} \frac{\partial \psi_{i'm'n'}}{\partial x_p} \quad (17)$$

is continuous for even l , particularly across material interfaces where σ_i usually changes. The derivation of the difference approximation will be shown only for the positive x direction as the other five terms follow a similar pattern.

From Figure 2 the expansion of $\psi_{i'm'n'}^-(y,z)$ for derivatives with respect to x is required and other differentials parallel to the surface are continuous. Thus

$$\begin{aligned} (c_{lmn,1}^{i'm'n'} \psi_{i'm'n'}^-)_{ijk} &= c_{lmn,1}^{i'm'n'} \left(\psi_{i'm'n'}^-(y,z) - \frac{\alpha_i}{2} \frac{\partial \psi_{i'm'n'}^-(y,z)}{\partial x} \right) - (y \frac{\partial}{\partial y} + z \frac{\partial}{\partial z}) \psi_{i'm'n'}^-(y,z) \\ &+ \left(\frac{\alpha_i^2}{8} \frac{\partial^2}{\partial x^2} + \frac{\alpha_i}{2} y \frac{\partial^2}{\partial x \partial y} + \frac{\alpha_i}{2} z \frac{\partial^2}{\partial x \partial z} + \frac{y^2}{2} \frac{\partial^2}{\partial y^2} + yz \frac{\partial^2}{\partial y \partial z} + \frac{z^2}{2} \frac{\partial^2}{\partial z^2} \right) c_{lmn,1}^{i'm'n'} \psi_{i'm'n'}^-(y,z) + \dots \end{aligned} \quad (18)$$

where $(\dots)_{ijk}$ denotes the value of what is in the brackets at point ijk and after expanding the parallel to mesh box surface derivatives about the midpoint of the cell side the above becomes

$$\begin{aligned} (c_{lmn,1}^{i'm'n'} \psi_{i'm'n'}^-)_{ijk} &= c_{lmn,1}^{i'm'n'} \psi_{i'm'n'}^-(y,z) - \frac{\alpha_i}{2} \frac{\partial c_{lmn,1}^{i'm'n'} \psi_{i'm'n'}^-(y,z)}{\partial x} - (y \frac{\partial}{\partial y} + z \frac{\partial}{\partial z}) (c_{lmn,1}^{i'm'n'} \psi_{i'm'n'}^-)_{i+\frac{1}{2}jk} \\ &+ \left(\frac{\alpha_i^2}{8} \frac{\partial^2}{\partial x^2} + \frac{\alpha_i}{2} y \frac{\partial^2}{\partial x \partial y} + \frac{\alpha_i}{2} z \frac{\partial^2}{\partial x \partial z} - \frac{y^2}{2} \frac{\partial^2}{\partial y^2} - yz \frac{\partial^2}{\partial y \partial z} - \frac{z^2}{2} \frac{\partial^2}{\partial z^2} \right) (c_{lmn,1}^{i'm'n'} \psi_{i'm'n'}^-)_{i+\frac{1}{2}jk} + \dots \end{aligned} \quad (19)$$

which integrates to, since by definition $S^{+1} = S_{jk}$

$$S_{jk} (c_{lmn,l}^{i'm'n'} \psi_{i'm'n'}^-)_{ijk} = \int_{S_{jk}} \left(c_{lmn,l}^{i'm'n'} \psi_{i'm'n'}^-(y,z) - \frac{\alpha_i}{2} \frac{\partial}{\partial x} c_{lmn,l}^{i'm'n'} \psi_{i'm'n'}^-(y,z) \right) dS^{+1} + \frac{S_{jk}}{8} \left(\alpha_i^2 \frac{\partial^2}{\partial x^2} - \frac{1}{3} (\beta_j^2 \frac{\partial^2}{\partial y^2} + \gamma_k^2 \frac{\partial^2}{\partial z^2}) \right) (c_{lmn,l}^{i'm'n'} \psi_{i'm'n'}^-)_{i+\frac{1}{2}jk} + \dots \quad (20).$$

Following a similar procedure for meshpoint $i+1jk$ yields

$$S_{jk} (c_{lmn,l}^{i'm'n'} \psi_{i'm'n'}^+)_{i+1jk} = \int_{S_{jk}} \left(c_{lmn,l}^{i'm'n'} \psi_{i'm'n'}^+(y,z) + \frac{\alpha_{i+1}}{2} \frac{\partial}{\partial x} c_{lmn,l}^{i'm'n'} \psi_{i'm'n'}^+(y,z) \right) dS^{+1} + \frac{S_{jk}}{8} \left(\alpha_{i+1}^2 \frac{\partial^2}{\partial x^2} - \frac{1}{3} (\beta_j^2 \frac{\partial^2}{\partial y^2} + \gamma_k^2 \frac{\partial^2}{\partial z^2}) \right) (c_{lmn,l}^{i'm'n'} \psi_{i'm'n'}^+)_{i+\frac{1}{2}jk} + \dots \quad (21).$$

Equation (20) is subtracted from relation (21) and, since the flux moments are continuous, on invoking condition (17) in the form

$$\frac{1}{(\sigma_l)_{ijk}} c_{lmn,p}^{i'm'n'} \frac{\partial \psi_{i'm'n'}^-(y,z)}{\partial x_p} = \frac{1}{(\sigma_l)_{i+1jk}} c_{lmn,p}^{i'm'n'} \frac{\partial \psi_{i'm'n'}^+(y,z)}{\partial x_p} \quad (22)$$

or

$$\frac{1}{(\sigma_l)_{i+1jk}} c_{lmn,l}^{i'm'n'} \frac{\partial \psi_{i'm'n'}^+(y,z)}{\partial x_1} = \frac{1}{(\sigma_l)_{ijk}} c_{lmn,l}^{i'm'n'} \frac{\partial \psi_{i'm'n'}^-(y,z)}{\partial x_1} + \left(\frac{1}{(\sigma_l)_{ijk}} - \frac{1}{(\sigma_l)_{i+1jk}} \right) c_{lmn,p}^{i'm'n'} \frac{\partial \psi_{i'm'n'}^-(y,z)}{\partial x_p} \quad (23)$$

with $p=2$ or 3 only and noting that derivatives parallel to the interface are continuous so the superscripts on the flux can be omitted then neglecting higher than second order derivatives, there results

$$\frac{1}{(\sigma_l)_{ijk}} \int_{S_{jk}} \frac{c_{lmn,l}^{i'm'n'} \partial \psi_{i'm'n'}^-(y,z)}{\partial x} dS^{+1} = \frac{2S_{jk}}{((\sigma_l)_{i+1jk} \alpha_{i+1} + (\sigma_l)_{ijk} \alpha_i)} \left(c_{lmn,l}^{i'm'n'} ((\psi_{i'm'n'}^-)_{i+1jk} - (\psi_{i'm'n'}^-)_{ijk}) + \frac{\alpha_{i+1}}{2} c_{lmn,p}^{i'm'n'} \left(1 - \frac{(\sigma_l)_{i+1jk}}{(\sigma_l)_{ijk}} \right) \frac{\partial (\psi_{i'm'n'}^-)_{i+\frac{1}{2}jk}}{\partial x_p} + \frac{c_{lmn,l}^{i'm'n'}}{8} \left(\alpha_i^2 \frac{\partial^2 (\psi_{i'm'n'}^-)_{i+\frac{1}{2}jk}}{\partial x_1} - \alpha_{i+1}^2 \frac{\partial^2 (\psi_{i'm'n'}^+)_{i+\frac{1}{2}jk}}{\partial x_1} \right) + \dots \right) \quad (24).$$

So that after including all terms as implied by equations (13) and (16)

$$\frac{1}{(\sigma_l)_{ijk}} \int_{S_{jk}} c_{lmp}^{i'm'n'} \frac{\partial \psi_{i'm'n'}(y,z)}{\partial x_p} dS^{s+1} = \frac{2S_{jk}}{((\sigma_l)_{i+1,jk} \alpha_{i+1} + (\sigma_l)_{ijk} \alpha_i)} \left(c_{lmi,1}^{i'm'n'} ((\psi_{i'm'n'})_{i+1,jk} - (\psi_{i'm'n'})_{ijk}) + \frac{(\alpha_{i+1} + \alpha_i)}{2} c_{lmi,p}^{i'm'n'} \frac{\partial (\psi_{i'm'n'})_{i+\frac{1}{2},jk}}{\partial x_p} + \frac{c_{lmi,1}^{i'm'n'}}{8} (\alpha_i^2 \frac{\partial^2 (\psi_{i'm'n'})_{i+\frac{1}{2},j}}{\partial x_1} - \alpha_{i+1}^2 \frac{\partial^2 (\psi_{i'm'n'})_{i+\frac{1}{2},j}}{\partial x_1}) + \dots \right) \quad (25)$$

A numerical approximation is consequently required for

$$\frac{\partial (\psi_{lmn})_{i+\frac{1}{2},jk}}{\partial x_p}$$

and this can be made to second order from the average on each side of the interface. Thus

$$\frac{\partial (\psi_{lmn})_{i+\frac{1}{2},jk}}{\partial y} = \frac{2(\alpha_i ((\psi_{lmn})_{i+1,j+k} - (\psi_{lmn})_{i+1,j-k}) + \alpha_{i+1} ((\psi_{lmn})_{ij+k} - (\psi_{lmn})_{ij-k}))}{(\alpha_{i+1} + \alpha_i)(\beta_{j-1} + 2\beta_j + \beta_{j+1})} + \dots \quad (26)$$

and equation (12) can now be expressed in difference form since in the usual approximations second order contributions like the second term in expression (14) and the third on the right hand side of relation (25) are neglected. In this derivation they have been retained for work in a later chapter on mesh effects but will not figure in the basic transport solution.

To obtain the difference equation equivalent of relation (12) assuming there is no external source $Q(\mathbf{r}, \Omega)$ first define

$$D_{i+\frac{1}{2},jk}^i = \frac{2S_{ij}}{(\sigma_{i+1,jk} \alpha_{i+1} + \sigma_{i,jk} \alpha_i)}, \Delta^{zi}(\psi_{lmn})_{ijk} = ((\psi_{lmn})_{i\pm 1,jk} - (\psi_{lmn})_{ijk}) \text{ and}$$

$$\Delta^{zj}(\psi_{lmn})_{ijk} = \pm \frac{(\alpha_i ((\psi_{lmn})_{i\pm 1,j+k} - (\psi_{lmn})_{i\pm 1,j-k}) + \alpha_{i+1} ((\psi_{lmn})_{ij+k} - (\psi_{lmn})_{ij-k}))}{(\beta_{j-1} + 2\beta_j + \beta_{j+1})} \quad (27)$$

with similar definitions for the other directions then

$$\begin{aligned} & -c_{lmi,1}^{i'm'n'} \frac{D_{i+\frac{1}{2},jk}^i}{(2l'+1)} \left(c_{lmi,1}^{i'm'n'} \Delta^{\pm 1} + c_{lmi,p}^{i'm'n'} \Delta^{\pm 1p'} \right) (\psi_{i'm'n'})_{ijk} \\ & -c_{lmi,2}^{i'm'n'} \frac{D_{ij+\frac{1}{2},k}^i}{(2l'+1)} \left(c_{lmi,2}^{i'm'n'} \Delta^{\pm 2} + c_{lmi,p}^{i'm'n'} \Delta^{\pm 2p'} \right) (\psi_{i'm'n'})_{ijk} \\ & -c_{lmi,3}^{i'm'n'} \frac{D_{ijk+\frac{1}{2}}^i}{(2l'+1)} \left(c_{lmi,3}^{i'm'n'} \Delta^{\pm 3} + c_{lmi,p}^{i'm'n'} \Delta^{\pm 3p'} \right) (\psi_{i'm'n'})_{ijk} + V_{ijk} (2l'+1) \sigma_l (\psi_{lmn})_{ijk} = 0 \end{aligned} \quad (28)$$

on neglecting second orders and with $l=0,2,\dots,N-1$, $m=0,1,2,\dots,l$. The foregoing are the standard equations solved for the second order system obtained by eliminating odd l moments

Chapter 4 BOUNDARY CONDITIONS

Two types of boundary are usually allowed, vacuum and reflection. Using variational⁽⁴⁾ principles the vacuum boundary conditions for an expansion to N can be shown to be

$$\int_{n.\Omega \leq 0} P_l^m(\cos\theta) \begin{pmatrix} \cos m\phi \\ \sin m\phi \end{pmatrix} \sum_{i=0,2,4,\dots}^{N-1} (2l+1) \sum_{m=0,1,2,\dots}^l P_i^m(\cos\theta) \begin{pmatrix} \psi_{i,m}(\mathbf{r}) \cos(m\phi) \\ + \gamma_{i,m}(\mathbf{r}) \sin(m\phi) \end{pmatrix} d\Omega = 0 \quad (29).$$

for $l=0,2,4,\dots,N-1$, $m=0,1,2,\dots,l$.

However because in a mesh centered approximation flux values on the surface must be obtained by extrapolation, the implementation of the above constraint is very complicated and normally the problem is extended by a few mean free paths of the boundary material but converted to pure absorber so that effectively all moments are zero at the new edges.

At a reflective boundary flux moments are zero or have zero gradient depending on whether the spherical harmonic

$$P_l^m(\cos\theta) \begin{pmatrix} \cos m\phi \\ \sin m\phi \end{pmatrix} \quad (30)$$

is odd or even respectively across the boundary.

The approximate vacuum and accurate reflective conditions can be summarized as

$$\frac{1}{3\sigma_t} \mathbf{n} \cdot \nabla \begin{pmatrix} \psi_{lm} \\ \gamma_{lm} \end{pmatrix} = -\lambda \begin{pmatrix} \psi_{lm} \\ \gamma_{lm} \end{pmatrix} \quad (31),$$

a similar relation to that used in Diffusion theory. For a vacuum and odd parity across a reflective boundary λ is set to a large number (10^{10}) and for reflection zero.

The numerical implementation follows the procedure used at material interfaces except that instead of involving flux values on both sides of the interface $\psi_{i,m}^-(y,z)$ in expression (20) is replaced by

$$\frac{1}{3\sigma_t \lambda} \frac{\partial \psi_{i,m}^-(y,z)}{\partial x} \quad (32)$$

leading to a modified equation (24) as shown below.

$$\frac{1}{(\sigma_i)_{ijk}} \int_{S_{jk}} \frac{c_{lmn,p}^{i\bar{m}\bar{n}} \partial \psi_{i\bar{m}\bar{n}}^-(y,z)}{\partial x_p} dS = \frac{3S_y \lambda}{(1+1.5\lambda(\sigma_i)_{ijk} \alpha_i)} \left(\begin{aligned} & -c_{lmn,l}^{i\bar{m}\bar{n}} (\psi_{i\bar{m}\bar{n}}^-)_{ijk} + \frac{\alpha_i}{2} c_{lmn,q}^{i\bar{m}\bar{n}} \frac{\partial (\psi_{i\bar{m}\bar{n}}^-)_{i+\frac{1}{2}jk}}{\partial x_q} + \frac{\alpha_i^2}{8} c_{lmn,l}^{i\bar{m}\bar{n}} \frac{\partial^2 (\psi_{i\bar{m}\bar{n}}^-)_{ijk}}{\partial x^2} \\ & - \frac{c_1^{i\bar{m}\bar{n}}}{24} \left(\beta_j^2 \frac{\partial^2 (\psi_{i\bar{m}\bar{n}}^-)_{i+\frac{1}{2}j}}{\partial y^2} + \gamma_k^2 \frac{\partial^2 (\psi_{i\bar{m}\bar{n}}^-)_{i+\frac{1}{2}j}}{\partial z^2} \right) + \dots \end{aligned} \right) \quad (33)$$

where $q=2$ or 3 and the approximation to derivatives parallel to the surface becomes from relation.(26) in the y direction for example.

$$\frac{\partial (\psi_{lmn}^-)_{i+\frac{1}{2}jk}}{\partial y} = \frac{2(\psi_{lmn}^-)_{ij+1k} - (\psi_{lmn}^-)_{ij-1k}}{(\beta_{j-1} + 2\beta_j + \beta_{j+1})} \quad (34).$$

The reason for the simplified vacuum condition is that it corresponds to the usual Diffusion theory constraint, $\frac{1}{3\sigma_0} \mathbf{n} \cdot \nabla \phi = -\lambda \phi$,

where ϕ is the flux and so the same coding can be used for the transport solution.

For equation (28) at a boundary in the x direction $D_{i+\frac{1}{2}jk}$ can be taken straightforwardly from relation (33) to be

$$D_{i+\frac{1}{2}jk} = \frac{3\lambda S_y}{(1+1.5\lambda\sigma_{ijk} \alpha_i)} \quad (35)$$

with similar expressions for the other axes.

Chapter 5 TRANSPORT THEORY SOLUTION ALGORITHM.

The principle of the method is straightforward and, as mentioned in Chapter 2, makes use of established techniques for solving the diffusion equation to provide an efficient algorithm. As can be seen from Appendix 2 the lm term looks very similar to the diffusion equation except that different constants multiply the second order differentials. Thus since transport solutions may be regarded as corrections to diffusion theory the solution procedure of taking other moments in the equation as an external source suggests itself. This is in fact the algorithm implemented and, beginning with a guess of moment values, the equations are solved for all moments in the highest energy group in the order $l=0,2,\dots,N-1$, $m=0,1,2,\dots,l$ using latest values in the enlarged source term. The moments are then calculated for the second highest energy and this process repeats until all groups have been evaluated. Eigenvalue adjustment follows by balancing the fission source from iteration to iteration. Thus if $(\psi_{00}^n)_{ijk}$ denotes the zero'th flux moment column vector at point ijk from iteration n then

$$k_{n+1} = k_n \frac{\sum_{ijk} (v\sigma_f \psi_{00}^{n+1})_{ijk} (v\sigma_f \psi_{00}^{n+1})_{ijk}}{\sum_{ijk} (v\sigma_f \psi_{00}^{n+1})_{ijk} (v\sigma_f \psi_{00}^n)_{ijk}} \quad (36).$$

Hence if scalar fluxes increase from the n th to $n+1$ th iteration so does k thus reducing the new fission source as is required for convergence.

The recalculation of moments continues until the eigenvalue and point fission sources are changing by less than preset accuracy criteria.

Moment values are calculated by line overrelaxation⁽¹⁾ and this gives an efficient solution algorithm.

Chapter 6. MESH CORRECTION TERMS

The mesh effect is known to be small for Diffusion theory⁽¹⁾ so the assumption has been made that this will be the case for Transport theory. Hence it is only necessary to include the correction for the scalar flux that is $\psi_{00}(\mathbf{r})$. Thus after converging the transport solution the calculation continues keeping higher moments constant and only solving for the scalar flux with the correction term, taken from the

second order terms for the zeroth moment in expressions (14) and (25)

$$\begin{aligned}
 & -\frac{V}{24}(\sigma_o)_{ijk}(\alpha_i^2 \frac{\partial^2}{\partial x^2} + \beta_j^2 \frac{\partial^2}{\partial y^2} + \gamma_k^2 \frac{\partial^2}{\partial z^2})(\psi_{00})_{ijk} \\
 & -\frac{1}{8} \left(\begin{aligned}
 & D_{i+\frac{1}{2}jk} \frac{\partial^2}{\partial x^2} (\alpha_{i+1}^2 (\psi_{00})_{i+\frac{1}{2}jk}^+ - \alpha_i^2 (\psi_{00})_{i+\frac{1}{2}jk}^-) - D_{i-\frac{1}{2}jk} \frac{\partial^2}{\partial x^2} (\alpha_i^2 (\psi_{00})_{i-\frac{1}{2}jk}^+ - \alpha_{i-1}^2 (\psi_{00})_{i-\frac{1}{2}jk}^-) \\
 & + D_{ij+\frac{1}{2}k} \frac{\partial^2}{\partial y^2} (\beta_{j+1}^2 (\psi_{00})_{ij+\frac{1}{2}k}^+ - \beta_j^2 (\psi_{00})_{ij+\frac{1}{2}k}^-) - D_{ij-\frac{1}{2}k} \frac{\partial^2}{\partial y^2} (\beta_j^2 (\psi_{00})_{ij-\frac{1}{2}k}^+ - \beta_{j-1}^2 (\psi_{00})_{ij-\frac{1}{2}k}^-) \\
 & + D_{ijk+\frac{1}{2}} \frac{\partial^2}{\partial z^2} (\gamma_{k+1}^2 (\psi_{00})_{ijk+\frac{1}{2}}^+ - \gamma_k^2 (\psi_{00})_{ijk+\frac{1}{2}}^-) - D_{ijk-\frac{1}{2}} \frac{\partial^2}{\partial z^2} (\gamma_k^2 (\psi_{00})_{ijk-\frac{1}{2}}^+ - \gamma_{k-1}^2 (\psi_{00})_{ijk-\frac{1}{2}}^-)
 \end{aligned} \right) \quad (37).
 \end{aligned}$$

Then neglecting higher moments than the zeroth formula (25) gives, assuming second orders are small, for the x direction

$$\begin{aligned}
 \frac{\partial(\psi_{00})_{i+\frac{1}{2}jk}^-}{\partial x} &= \frac{(\sigma_1)_{ijk} D_{i+\frac{1}{2}jk}}{S_{jk}} ((\psi_{00})_{i+1jk} - (\psi_{00})_{ijk}), \\
 \frac{\partial(\psi_{00})_{i-\frac{1}{2}jk}^+}{\partial x} &= \frac{(\sigma_1)_{ijk} D_{i-\frac{1}{2}jk}}{S_{jk}} ((\psi_{00})_{ijk} - (\psi_{00})_{i-1jk})
 \end{aligned} \quad (38)$$

so that to second order

$$\begin{aligned}
 \frac{\partial^2(\psi_{00})_{ijk}}{\partial x^2} &= \frac{(\sigma_1)_{ijk}}{\alpha_i S_{jk}} (D_{i+\frac{1}{2}jk} ((\psi_{00})_{i+1jk} - (\psi_{00})_{ijk}) + D_{i-\frac{1}{2}jk} ((\psi_{00})_{ijk} - (\psi_{00})_{i-1jk})) \\
 &= \Delta_x^2 (\psi_{00})_{ijk}
 \end{aligned} \quad (39)$$

say.

Thus the final expression for the mesh correction term is

$$\begin{aligned}
 & -\frac{V}{24}(\sigma_o)_{ijk}(\alpha_i^2 \Delta_x^2 + \beta_j^2 \Delta_y^2 + \gamma_k^2 \Delta_z^2)(\psi_{00})_{ijk} \\
 & -\frac{1}{8} \left(\begin{aligned}
 & D_{i+\frac{1}{2}jk} \Delta_x^2 (\alpha_{i+1}^2 (\psi_{00})_{i+\frac{1}{2}jk} - \alpha_i^2 (\psi_{00})_{i+\frac{1}{2}jk}) - D_{i-\frac{1}{2}jk} \Delta_x^2 (\alpha_i^2 (\psi_{00})_{i-\frac{1}{2}jk} - \alpha_{i-1}^2 (\psi_{00})_{i-\frac{1}{2}jk}) \\
 & + D_{ij+\frac{1}{2}k} \Delta_y^2 (\beta_{j+1}^2 (\psi_{00})_{ij+\frac{1}{2}k} - \beta_j^2 (\psi_{00})_{ij+\frac{1}{2}k}) - D_{ij-\frac{1}{2}k} \Delta_y^2 (\beta_j^2 (\psi_{00})_{ij-\frac{1}{2}k} - \beta_{j-1}^2 (\psi_{00})_{ij-\frac{1}{2}k}) \\
 & + D_{ijk+\frac{1}{2}} \Delta_z^2 (\gamma_{k+1}^2 (\psi_{00})_{ijk+\frac{1}{2}} - \gamma_k^2 (\psi_{00})_{ijk+\frac{1}{2}}) - D_{ijk-\frac{1}{2}} \Delta_z^2 (\gamma_k^2 (\psi_{00})_{ijk-\frac{1}{2}} - \gamma_{k-1}^2 (\psi_{00})_{ijk-\frac{1}{2}})
 \end{aligned} \right) \quad (40).
 \end{aligned}$$

There are no external boundary terms as gradients are zero for reflection and fluxes zero at a vacuum surface.

Chapter 7. TEST CASES

Sample problems have been taken from the Transport Theory benchmark exercise⁽⁶⁾ carried out some years ago.

7.1 Small FBR Problem

The problem examined was the small FBR in XYZ geometry shown in Figure 3 with the cross section data specified in Appendix 3. Tables 1 and 2 show the eigenvalues for the full and half mesh size cases with and without mesh correction on the zeroth moment. It seems plausible based on diffusion theory studies^(1,7) and previous PN calculations⁽⁸⁾ to assume transport eigenvalues vary as the square of the mesh size as the system solved is second order. This hypothesis appears to be borne out by Table 1 where the extrapolated zero mesh value is very close to the half mesh corrected value and the result from the Monte Carlo code MVP⁽⁹⁾. In fact the agreement with MVP is very good for the half mesh corrected case and this is extremely encouraging given that the Monte Carlo solution is of course based on tracking individual neutrons on a probabilistic basis by utilizing the computer pseudo-random number generator, in complete contrast to the deterministic approach of the spherical harmonics approximation.

Table 1 Eigenvalues for the Small FBR Control Rod Out

	full mesh	Half mesh	Zero mesh
Transport theory uncorrected	0.97647	0.97440	0.97371
Transport theory mesh corrected	0.97412	0.97359	
MVP Monte Carlo			0.9732 ⁽⁶⁾ ±0.0005

Table 2 Eigenvalues for the Small FBR Control Rod Half In

	full mesh	Half mesh	Zero mesh
Transport theory uncorrected	0.96380	0.96077	0.95977
Transport theory mesh corrected	0.96028	0.95956	
MVP Monte Carlo			0.9593 ⁽⁶⁾ ±0.0004

7.2 Large FBR Problem

This problem illustrated in Figure 4 has a great deal of radial heterogeneity. Results obtained for the control rod in and out cases are shown in Tables 3 and 4 respectively and again the assumed mesh squared dependence and the half mesh corrected case give good agreement with the Monte Carlo values from MVP and VIM. Two codes have been quoted because there appear to be some significant variations in their results.

Table 3 Eigenvalues for the Large FBR Control Rod In

	full mesh	Half mesh	Zero mesh
Transport theory uncorrected	0.97681	0.97301	0.97159
Transport theory mesh corrected	0.97215	0.97140	
MVP ⁽⁶⁾ Monte Carlo			0.9712±0.0005
VIM ⁽⁶⁾ Monte Carlo			0.9709±0.0003

Table 4 Eigenvalues for the Large FBR Control Rod Out

	full mesh	Half mesh	Zero mesh
Transport theory uncorrected	1.00376	1.00189	1.00127
Transport theory mesh corrected	1.00135	1.00098	
MVP ⁽⁶⁾ Monte Carlo			0.9998±0.0007
VIM ⁽⁶⁾ Monte Carlo			1.0006±0.0003

Chapter 8 CONCLUSIONS

A technique for eliminating second order mesh errors has been extended from Diffusion Theory⁽¹⁾ to Transport Equation solutions based on an expansion of the flux in unnormalised spherical harmonics. Because the mesh corrections, though important, are relatively small they need only be applied to the zeroth moment or scalar flux. Problem results show that the solution follows the mesh squared dependency rule found in Diffusion theory.

Fluxes can now be calculated for a zero mesh because second order effects have been removed so that there are no canceling errors of this order. Hence discrepancies with experiment must arise from basic cross section data or the adjustment for homogenization usually based on some kind of cell treatment⁽¹⁰⁾.

The use of simplified vacuum boundary conditions comes from a technical difficulty only and the actual equations could be implemented. A more serious problem⁽¹¹⁾ arises with low density regions where, because the elimination of odd moments implies division by a small cross section as indicated by equation (17), a spurious non-physical flat flux solution can arise. Various methods⁽¹¹⁾ have been proposed to overcome this difficulty but the most promising approach appears to be to use the first order equations in the low density or void region and implement some merging procedure to the rest of the problem which is solved by the efficient algorithms available for the second order system. This task would be the next development of the method.

REFERENCES

- (1) Fletcher J. K., An Investigation of Discretization Errors for Mesh Centered Finite Difference Approximations: PNC TN9410 96-277 (1996)
- (2) Fletcher J. K., MARC/PN. A Computer Code to Solve the Multigroup Neutron Transport Equation.: RTS-002(88) AEA Technology (1988)
- (3) Davison B., Neutron Transport Theory.: Oxford U P, Oxford (1957)
- (4) Ackroyd R. T. et al, Recent Developments in Finite Element Methods for Neutron Transport Theory.: Advances in Nuclear Science and Technology. Vol. 19, Plenum Press New York and London (1987)
- (5) Kobayashi K. et al, The Spherical Harmonics Method for the Multigroup Transport Equation in x-y Geometry: Ann. Nuc. Energy 13 12 pp 663-678 (1986)
- (6) Takeda T., Ikeda H., 3-D Neutron Transport Benchmarks.: NEACRP-L-330 (1991)
- (7) Kato Y., Spatial Mesh Effects in Three Dimensional x-y-z Neutron Diffusion Calculations in Fast Breeders Reactors: Nuc. Sci. & Eng. 104 402-411 (1990)
- (8) Fletcher J. K.,: The Use of Supercomputers for Reactor Physics Calculations.: Proceeding SNA Conference., Mito (1990)
- (9) Mori T., Nakagawa J.: MVP/GMVP: General Purpose Monte Carlo Codes for Neutron and Photon Transport Calculations based on Continuous Energy and Multigroup Methods: JAERI-Data/Code 94-007 (1994)
- (10) Nakagawa M., Tsuchihashi K., SLAROM A Code for Cell Homogenization of Fast Reactors: JAERI 1294 (1984)

- (11) Ackroyd R. T., Ryait N., Iteration and Extrapolation Methods for the Approximate Solution of the Even-parity Transport Equation for Systems with Voids: Ann. Nuc. Energy **16** 1 pp1-32 (1989)

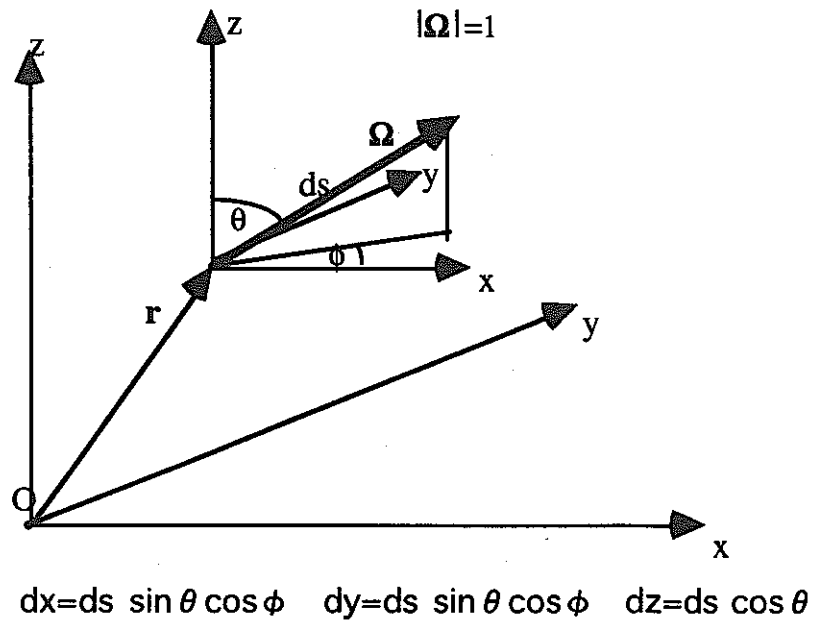


Figure 1 Definition of r and Ω

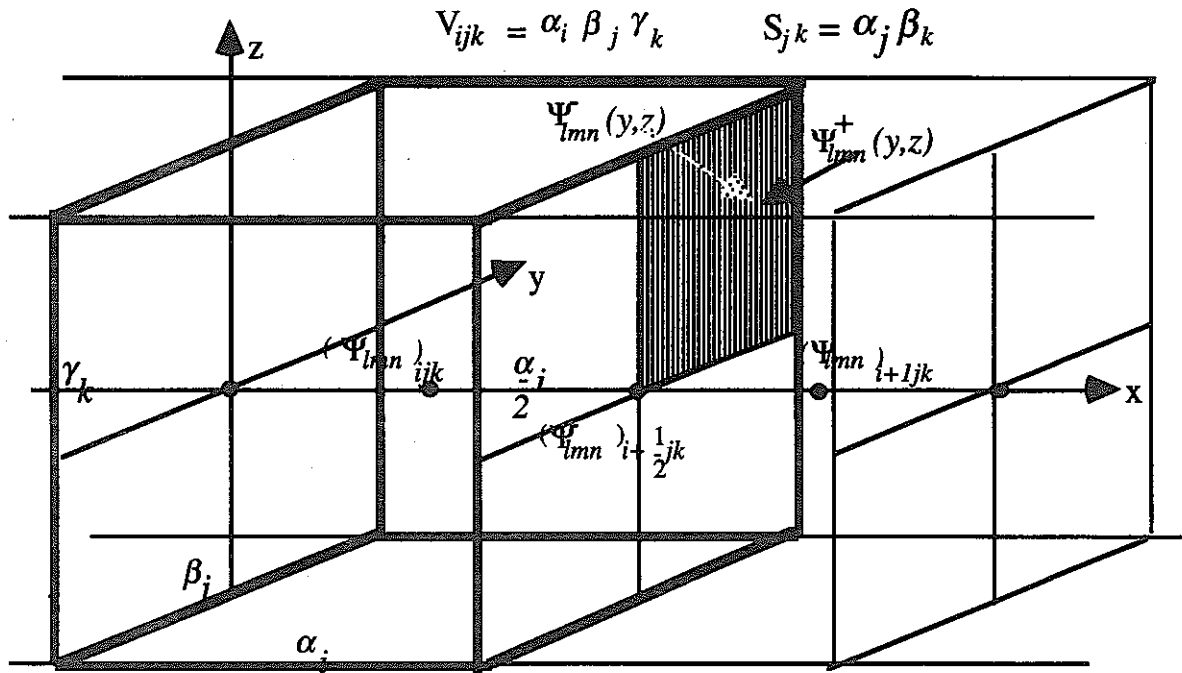
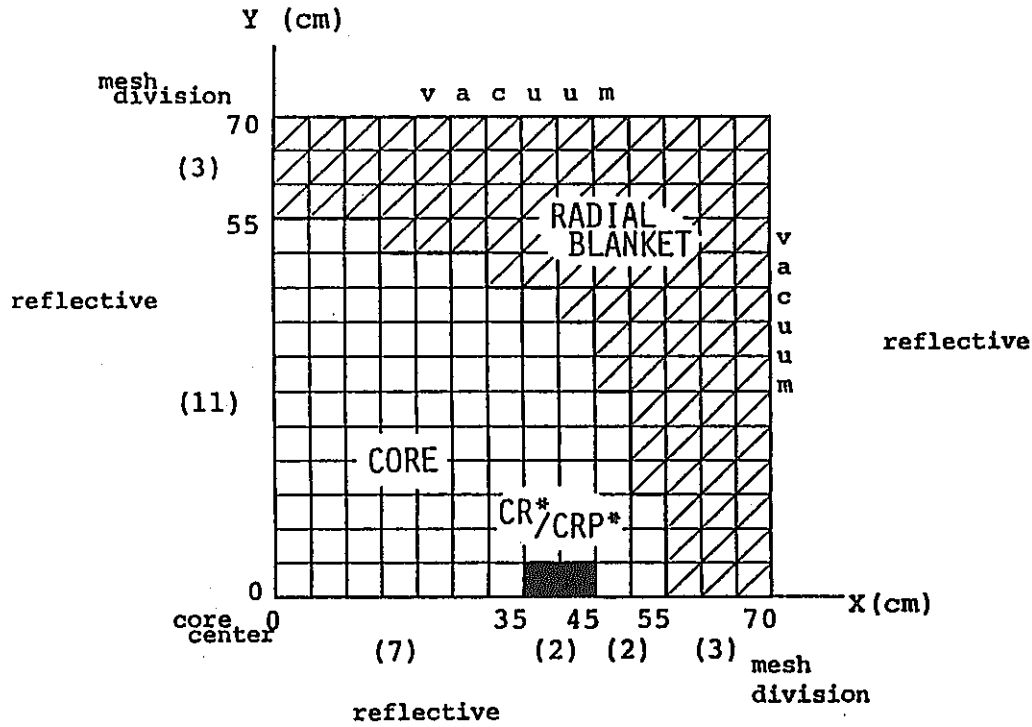
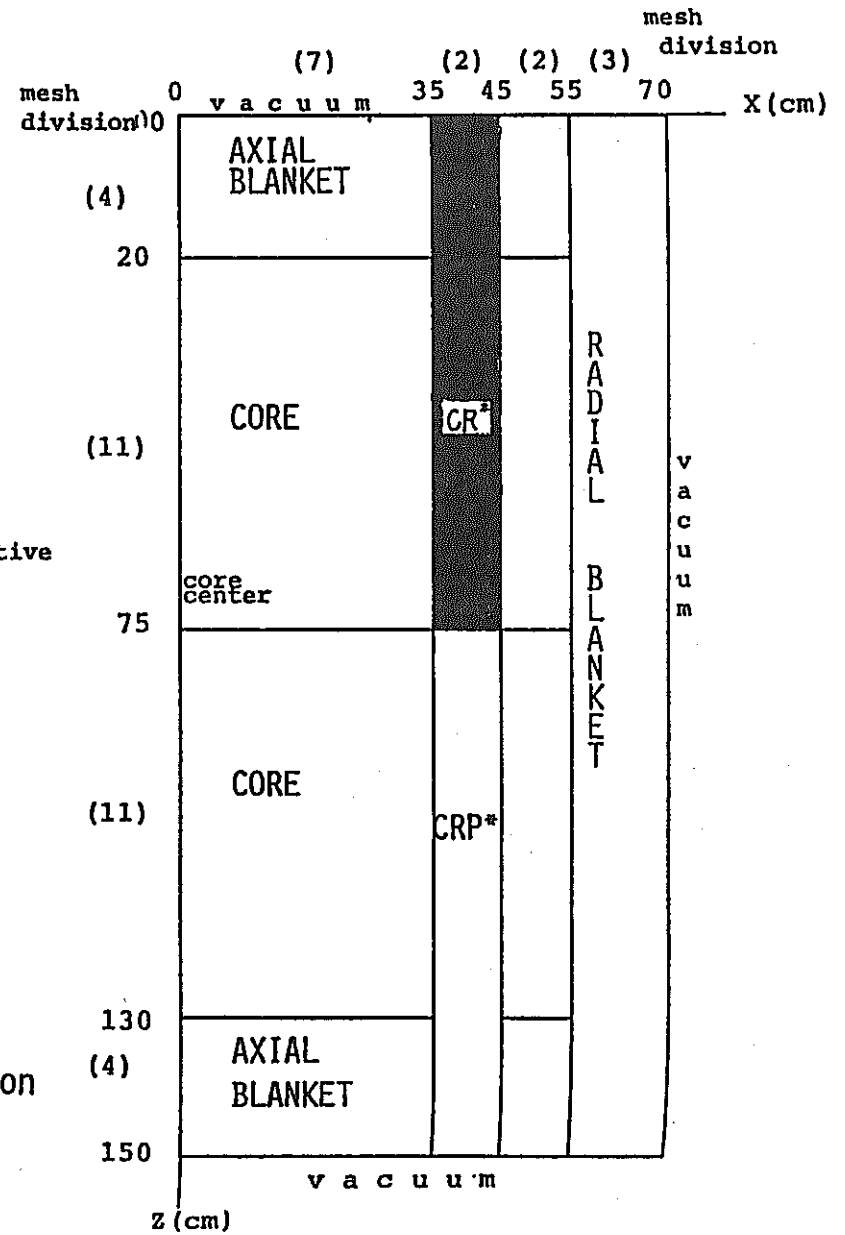


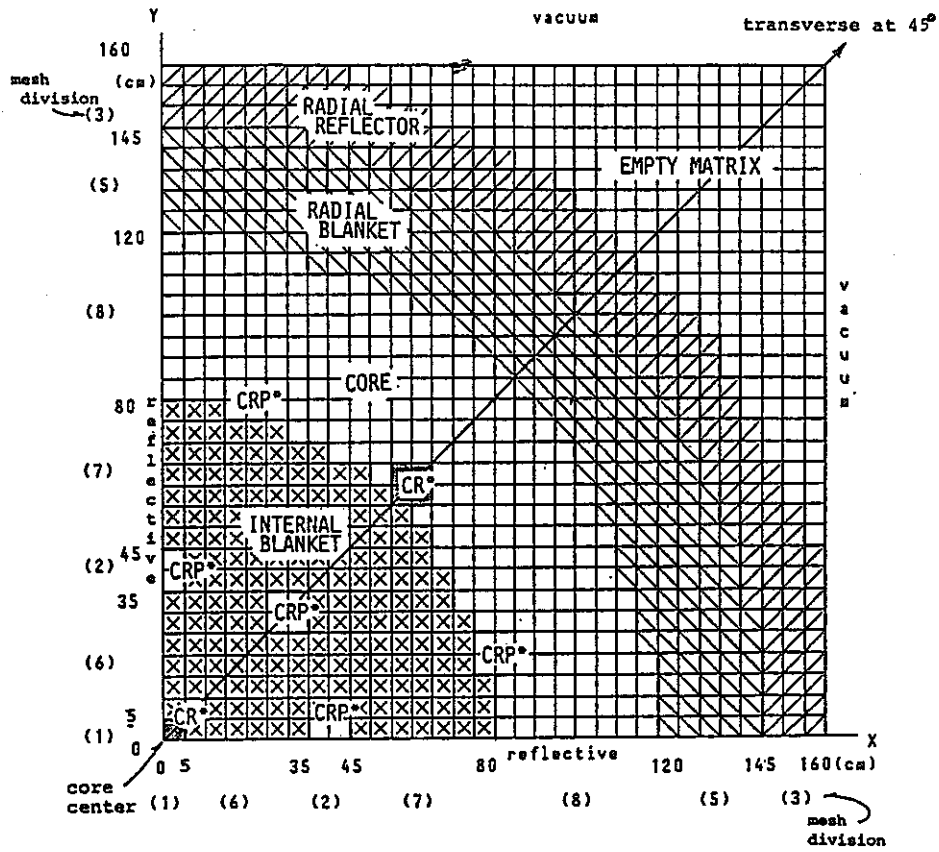
Figure 2 A typical mesh in XYZ Geometry

Figure 3 Small FBR Test Problem



*CR : Control rod
 CRP: Na filled control rod position





*CR : Control rod
 CRP: Na filled control rod position

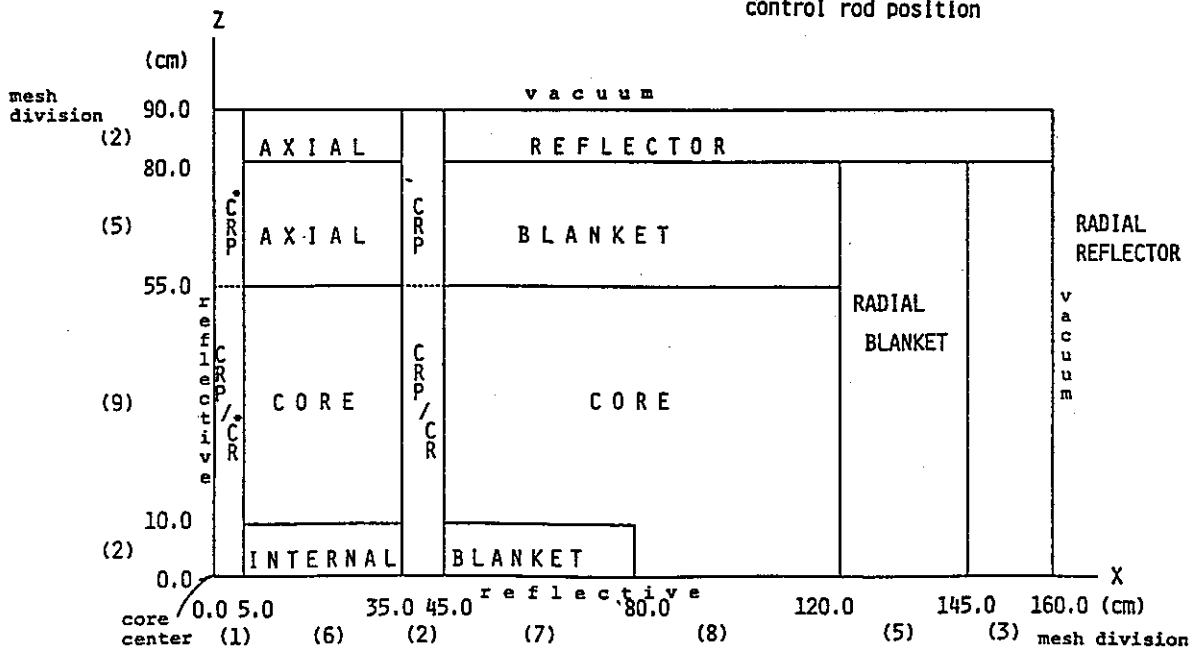


Figure 4 Large FBR Test Problem

APPENDIX 1. FORTRAN CODE TO CALCULATE THE SECOND ORDER SYSTEM

```

SUBROUTINE MOMENT(A, IA)
COMMON /BASIC/NG,NDSCAT,NUPSCAT,IMAX,KMAX,JMAX,IPI,IPK,IPJ,
1LCC,NMS,NZS,IPIS,IPMS,IPZS,IPLB,IPRB,NPTS,ITOP,MAXC,NERR,
2LOCCA,LOCI,NXSM,MAXI,NT1,NT2,NT3,NT4,NT5,ACC1,ACC2,BC(6),
3NAMGM,NPN,LOCD,LOCC,LOCF,LPN,LOCIC
COMMON /STORE/CH(1)
DIMENSION C(6,15),IC(6,15),W(12),IW(12),Y(12),IY(12),IDV(3,3)
1,A(1),IA(1)
DATA IDV/1,2,2,1,2,2,1,1,3/
LOC2=1
LOC3=20001
NMOM=(NPN*(NPN+1))/2
LEND=3*NMOM
LOCD=ITOP-LEND
LOCT=LOCD
DO 8 L=1,NPN,2
NM=1
DO 8 M=1,L
DO 7 NN=1,NM
LP=L-1
MP=M-1
WRITE(6,100) LP,MP,NN
100 FORMAT(1X,'L=',I4,' M=',I4,I4,' MOMENT EQUATION')
DO 1 I=1,15
DO 1 J=1,6
C(J,I)=0.
1 IC(J,I)=0.
CALL COEF(W,IW,L-1,M-1,NN)
DO 5 J=1,6
LL=L+2*((J-1)/3)-2
MM=M+J-3*((J-1)/3)-3
IF(LL.LT.0.OR.MM.LT.0.OR.MM.GT.LL) GO TO 5
DO 4 K=1,2
IF(K.EQ.2.AND.MM.EQ.0) GO TO 4
XL=LL
XL=1./(2.*XL+1)
CALL COEF(Y,IY,LL,MM,K)
JW=J+(K-1)*6
LW=IW(JW)
DO 2 JJ=1,6
LLL=LL-1+2*((JJ-1)/3)
MMM=MM-2+JJ-3*((JJ-1)/3)
IF(LLL.LT.0.OR.LLL.GT.NPN.OR.MMM.LT.0.OR.MMM.GT.LLL) GO TO 2
LOC=(J-1)/3+(JJ-1)/3*2+J+JJ-1
LY1=IY(JJ)
LY2=IY(JJ+6)
LWY1=IDV(LW,LY1)
LWY2=IDV(LW,LY2)+3
C(LWY1,LOC)=W(JW)*Y(JJ)*XL+C(LWY1,LOC)
C(LWY2,LOC)=W(JW)*Y(JJ+6)*XL+C(LWY2,LOC)
IF(W(JW).NE.0..AND.Y(JJ).NE.0.)
1IC(LWY1,LOC)=IW(JW)*IY(JJ)
IF(W(JW).NE.0..AND.Y(JJ+6).NE.0.)
1IC(LWY2,LOC)=IW(JW)*IY(JJ+6)
2 CONTINUE
3 CONTINUE
4 CONTINUE
5 CONTINUE
DO 6 J=1,15
LL=L+2*((J-1)/5)-3
MM=M+J-5*((J-1)/5)-4

```

```

DO 6 K=1,2
I=3*(K-1)+1
II=3*K
IF(C(I,J).NE.0..OR.C(I+1,J).NE.0..OR.C(I+2,J).NE.0.) THEN
101 WRITE(6,101) LL,MM,K,(IC(KK,J),C(KK,J),KK=I,II)
FORMAT(4X,3I4,3(I4,E14.6))
IF(LP.EQ.LL.AND.MP.EQ.MM.AND.NN.EQ.K) THEN
CALL EQVEC(C(I,J),CH(LOCT),3)
LOCT=LOCT+3
ELSE
CALL EQVEC(C(I,J),A(LOC2),3)
CALL EQVEC(IC(I,J),IA(LOC2),3)
LOC2=LOC2+3
LOCF=(LL*(LL-1))/2+MAX0(2*MM-1,0)+K
IA(LOC3)=LOCF
LOC3=LOC3+1
ENDIF
ENDIF
6 CONTINUE
IA(LOC3)=-1
7 LOC3=LOC3+1
8 NM=2
LOCC=LOCD-LOC2
CALL EQVEC(A,CH(LOCC),LOC2)
LOCIC=LOCC-LOC2
CALL EQVEC(IA,CH(LOCIC),LOC2)
LENF=LOC3-20000
LOCF=LOCIC-LENF
CALL EQVEC(IA(20001),CH(LOCF),LENF)
ITOP=LOCF
RETURN
END
SUBROUTINE COEF(W,IW,L,M,I)
DIMENSION W(12),IW(12),IS(2)
DATA IS/1,-1/
DO 1 J=1,6,3
IW(J)=I
IW(J+2)=I
IW(J+1)=3
IW(J+7)=3
IW(J+8)=3-I
1 IW(J+6)=3-I
W(1)=1
W(2)=2*(L-M)*(2-I)
W(3)=- (L-M)*(L-M-1)*IS(I)
W(4)=-1
W(5)=2*(L+M+1)*(2-I)
W(6)=(L+M+1)*(L+M+2)*IS(I)
W(7)=-IS(I)
W(8)=2*(L-M)*(I-1)
W(9)=- (L-M)*(L-M-1)
W(10)=IS(I)
W(11)=2*(L+M+1)*(I-1)
W(12)=(L+M+1)*(L+M+2)
IF(M.EQ.1) THEN
W(1)=2.
W(4)=-2.
W(7)=0.
W(10)=0.
ENDIF
DO 2 J=1,12
2 W(J)=W(J)*0.5
RETURN
END

```

APPENDIX 2. P3 EQUATIONS FOR XYZ GEOMETRY

The L and M values below are given by the first two digits. For the third 1 signifies $\psi_m(\mathbf{r})$ and 2, $\gamma_m(\mathbf{r})$.

$\frac{\partial}{\partial x}$ is denoted by 1, $\frac{\partial}{\partial y}$ and $\frac{\partial}{\partial z}$ by 2 and 3 respectively. Second

order derivatives are products of these thus 6 implies $\frac{\partial^2}{\partial y \partial z}$ for the integers immediately preceding the coefficients.

L=	0	M=	0	1	MOMENT EQUATION				
	0	0	1	1	0.333333E+00	4	0.333333E+00	9	0.333333E+00
	2	0	1	1	-0.333333E+00	4	-0.333333E+00	9	0.666667E+00
	2	1	1	3	0.100000E+01	3	0.100000E+01	0	0.000000E+00
	2	1	2	6	0.100000E+01	6	0.100000E+01	0	0.000000E+00
	2	2	1	1	0.200000E+01	4	-0.200000E+01	0	0.000000E+00
	2	2	2	2	0.200000E+01	2	0.200000E+01	0	0.000000E+00
L=	2	M=	0	1	MOMENT EQUATION				
	0	0	1	1	-0.333333E+00	4	-0.333333E+00	9	0.666667E+00
	2	0	1	1	0.119048E+01	4	0.119048E+01	9	0.261905E+01
	2	1	1	3	0.714285E+00	3	0.714285E+00	0	0.000000E+00
	2	1	2	6	0.714285E+00	6	0.714285E+00	0	0.000000E+00
	2	2	1	1	-0.285714E+01	4	0.285714E+01	0	0.000000E+00
	2	2	2	2	-0.285714E+01	2	-0.285714E+01	0	0.000000E+00
L=	2	M=	1	1	MOMENT EQUATION				
	0	0	1	3	0.333333E+00	3	0.333333E+00	0	0.000000E+00
	2	0	1	3	0.238095E+00	3	0.238095E+00	0	0.000000E+00
	2	1	1	1	0.214286E+01	4	0.714286E+00	9	0.214286E+01
	2	1	2	2	0.714285E+00	2	0.714286E+00	0	0.000000E+00
	2	2	1	3	0.142857E+01	3	0.142857E+01	0	0.000000E+00
	2	2	2	6	0.142857E+01	6	0.142857E+01	0	0.000000E+00
L=	2	M=	1	2	MOMENT EQUATION				
	0	0	1	6	0.333333E+00	6	0.333333E+00	0	0.000000E+00
	2	0	1	6	0.238095E+00	6	0.238095E+00	0	0.000000E+00
	2	1	1	2	0.714286E+00	2	0.714285E+00	0	0.000000E+00
	2	1	2	1	0.714286E+00	4	0.214286E+01	9	0.214286E+01
	2	2	1	6	-0.142857E+01	6	-0.142857E+01	0	0.000000E+00
	2	2	2	3	0.142857E+01	3	0.142857E+01	0	0.000000E+00
L=	2	M=	2	1	MOMENT EQUATION				
	0	0	1	1	0.166667E+00	4	-0.166667E+00	0	0.000000E+00
	2	0	1	1	-0.238095E+00	4	0.238095E+00	0	0.000000E+00
	2	1	1	3	0.357143E+00	3	0.357143E+00	0	0.000000E+00
	2	1	2	6	-0.357143E+00	6	-0.357143E+00	0	0.000000E+00
	2	2	1	1	0.214286E+01	4	0.214286E+01	9	0.714286E+00
L=	2	M=	2	2	MOMENT EQUATION				
	0	0	1	2	0.166667E+00	2	0.166667E+00	0	0.000000E+00
	2	0	1	2	-0.238095E+00	2	-0.238095E+00	0	0.000000E+00
	2	1	1	6	0.357143E+00	6	0.357143E+00	0	0.000000E+00
	2	1	2	3	0.357143E+00	3	0.357143E+00	0	0.000000E+00
	2	2	2	1	0.214286E+01	4	0.214286E+01	9	0.714286E+00

APPENDIX 3 Cross Section Data for the XYZ Geometry Tests

There are 4 energy groups and 2 down scatters with cross sections given in the order

- 1) transport
- 2) removal, that is absorption plus scatter out of the group
- 3) ν -fission
- 4) down scatter in the order i to $i+1$, i to $i+2$ filled to a full band
- 5) fission spectrum
- 6) capture

Core

1.14568E-1	2.05177E-1	3.29381E-1	3.89810E-1				
4.41354E-2	9.73474E-3	8.79433E-3	2.74496E-2				
2.06063E-2	6.10571E-3	6.91403E-3	2.60689E-2				
3.47967E-2	1.88282E-3	6.20863E-3	7.07208E-7	9.92975E-4	0	0	0
0.583319	0.405450	0.011231	0.0				
7.45551E-3	3.52540E-3	7.80136E-3	2.74496E-2				

Radial Blanket

1.19648E-1	2.42195E-1	3.56476E-1	3.79433E-1				
5.05322E-2	1.15695E-2	8.06231E-3	1.58015E-2				
1.89496E-2	1.75265E-4	2.06978E-4	1.13451E-3				
4.04132E-2	2.68621E-3	9.57027E-3	1.99571E-7	1.27195E-3	0	0	0
0.583319	0.405450	0.011231	0.0				
7.43283E-3	1.99906E-3	6.79036E-3	1.58015E-2				

Axial Blanket

1.16493E-1	2.20531E-1	3.44544E-1	3.88356E-1				
4.48883E-2	1.00853E-2	7.03838E-3	1.34694E-2				
1.31770E-2	1.26026E-4	1.52380E-4	7.87302E-4				
3.73170E-2	2.21707E-3	8.59855E-3	6.68299E-7	1.68530E-3	0	0	0
0.583319	0.405450	0.011231	0.0				
5.35418E-3	1.48604E-3	5.35300E-3	1.34694E-2				

Axial Reflector

1.65613E-1	1.66866E-1	2.68633E-1	8.34911E-1				
4.99587E-2	6.04849E-3	3.62227E-3	4.36382E-3				
0.0	0.0	0.0	0.0				
4.84721E-2	8.46495E-4	5.64096E-3	6.57573E-7	2.41755E-3	0	0	0
0.0	0.0	0.0	0.0				

6.39154E-4 4.06876E-4 1.20472E-3 4.36383E-3

Radial Reflector

1.71748E-1 2.17826E-1 4.47761E-1 7.95199E-1
4.83959E-2 6.76283E-3 4.71626E-3 5.70263E-3
0.0 0.0 0.0 0.0
4.62307E-2 1.13217E-3 6.27100E-3 1.03831E-6 2.77126E-3 0 0 0
0.0 0.0 0.0 0.0
1.13305E-1 4.90793E-4 1.94500E-3 5.70263E-3

Control Rod

1.84333E-1 3.66121E-1 6.15527E-1 1.09486
4.99599E-2 4.75382E-2 9.59362E-2 4.76591E-1
0.0 0.0 0.0 0.0
4.37775E-2 2.06054E-4 2.98432E-2 8.71100E-7 7.66209E-3 0 0 0
0.0 0.0 0.0 0.0
5.97638E-3 1.76941E-2 8.82741E-2 4.76591E-1

Na filled Control Rod Position

6.58979E-2 1.09810E-1 1.86765E-1 2.09933E-1
1.84572E-2 3.66790E-3 1.46178E-3 1.07518E-3
0.0 0.0 0.0 0.0
1.76894E-2 4.57012E-4 3.55466E-3 1.77599E-7 1.01280E-3 0 0 0
0.0 0.0 0.0 0.0
3.10744E-4 1.13062E-4 4.48988E-4 1.07518E-3

Empty Matrix

1.36985E-2 1.69037E-2 3.12271E-2 6.29537E-2
4.11854E-3 4.29715E-4 3.16628E-4 4.95515E-4
0.0 0.0 0.0 0.0
3.95552E-3 8.80428E-5 3.91394E-4 7.72254E-8 1.77293E-4 0 0 0
0.0 0.0 0.0 0.0
7.49800E-5 3.82435E-5 1.39335E-4 4.95515E-4